The Potential of ERS for the Detection of Rossby Waves in the Northeast Atlantic

P. Cipollini, D. Cromwell, M.S. Jones, G.D. Quartly and P.G. Challenor

James Rennell Division, Southampton Oceanography Centre, Southampton, SO14 3ZH, UK

phone: +44-1703-596405, fax: +44-1703-596400

email: { cipo | ddc | msj | gdq | pc } soc.soton.ac.uk

URL: http://www.soc.soton.ac.uk

Abstract

We present observations of long-wavelength baroclinic Rossby waves near 34°N in the Northeast Atlantic ocean (east of the Mid-Atlantic Ridge) using ERS-1 Along-Track Scanning Radiometer sea surface temperature (SST) measurements and ERS-1 and TOPEX/POSEIDON sea surface height (SSH) altimeter data. Using the Fourier transforms of longitude-time diagrams of the zonal gradients of SST and SSH we locate the spectral components corresponding to westward wave propagation and estimate wavelength, period and propagation speed. The energy associated with the propagating waves in the region considered is distinctly higher than in the surrounding areas. The similarities between the properties of the SST and SSH zonal gradients are remarkable with the same propagating signals clearly observed in these fields. It is believed that the interaction between the Rossby waves and the Azores current could play a major role in the amplification of the waves themselves.

Keywords: Rossby waves, Azores Current, Altimetry, ATSR SST

1. Introduction

Oceanic Rossby wave propagation is one geophysical phenomenon whose study has dramatically benefited from space-based earth observation techniques. There are many reasons for their importance in oceanography. For example, they are responsible for the westward intensification of the oceanic circulation in ocean basins [Gill, 1982]. Moreover, the effects of ocean-atmosphere disturbances at eastern boundaries may be transmitted in a period of years (at extra-tropical latitudes) across the oceans as westward-travelling Rossby waves. These may affect western boundary currents which in turn have a strong influence on the climate over large areas [Jacobs et al. 1994].

Propagating Rossby waves perturb the density structure of the ocean, and produce a SSH signature according to whether the vertical integral of the density perturbation is negative (less dense), leading to increased sea surface height, or positive (more dense) causing reductions. The gradient of the resulting SSH signature is related to the surface velocity of the wave through geostrophy.

The advent of satellite altimetry has recently permitted the detection of long-wavelength (hundreds of kms) baroclinic Rossby waves through their (~10 cm or smaller) sea surface height (SSH) signature. The first satellite-borne altimeter with acceptable coverage and accuracy for such an application was Geosat, launched in 1985. Using Geosat data, Tokmakian and Challenor [1993] found evidence of Rossby wave propagation in the Azores region of the North Atlantic, although some part of the observed signal could be attributed to aliasing of the residual M2 tidal constituent, as pointed out by Schlax and Chelton [1994]. Recent altimeter missions have benefitted from superior tracking and orbit models; in addition, over recent years there have been many efforts to improve the accuracy of global tidal models [Andersen et al., 1995]. Here, we present the results from altimeters on 2 different satellites, which have different alias periods for the various residual tidal components, since they are in very different orbits.

As Rossby waves involve changes in the subsurface density field, there may be a manifestation in the Sea Surface Temperature (SST) field, depending on the extent to which surface and subsurface fields are coupled. If the SST gradient can be regarded as a proxy for the surface density gradient, and if this surface density gradient is correlated with the density gradient at depth, then perturbations in the density field should also be visible as perturbations in the SST field. Hence, it may be possible to observe baroclinic Rossby waves, through their effect on SST. A study of Rossby waves near the Hawaiian Islands by Van Woert and Price [1993] revealed westward propagating waves in the Goesat (altimetry) data, but not in the AVHRR (SST) data, whilst Halliwell et al. [1991] studying the Sargasso Sea did find similar propagating signals in the height and temperature fields. Here we focus our study on a particular region of the northeast Atlantic, using altimeter data from the TOPEX/POSEIDON (hereafter T/P) and ERS-1 satellites, and SST data from the Along-Track Scanning Radiometer (ATSR) on board ERS-1. Preliminary research by Cipollini et al. [1996a] had examined the strength of westward-propagating signals at various latitudes in the norteast Atlantic, and application of both Fourier and Radon Transforms had revealed a strong concentration of energy along 33°- 34°N, coinciding with the approximate location of the eastward flowing Azores Current. Illustrative results of this particular region are presented here, demonstrating how the same propagating features may be discerned in both SST and sea surface height data from 2 satellites in very different orbits.

2. Data processing

2.1 ATSR data processing

The ATSR data used in this study are the spatially averaged (0.5° in latitude and longitude) SST data (ASST), provided by the UK Rutherford Appleton Laboratory (RAL), covering the period January 1992 to December 1995. The ASST data are obtained by averaging the 1 km resolution brightness temperatures into 10-arcminute cells, and then obtaining a SST measurement for each cell. The ASST is then the average of the SSTs of the nine 10-arcminute cells.

The ATSR instrument has several design improvements over the AVHRR instruments which allow a more accurate point measurement of SST to be made. These improvements result in (1) more accurate calibration, (2) lower detector noise, and (3) a more accurate atmospheric correction [Závody et al., 1995]. Validation studies have shown that the ATSR can measure SST to a point relative accuracy of 0.3 K [Mutlow et al., 1994; Forrester and Challenor, 1995], twice the accuracy of the AVHRR [McClain et al., 1985].

Infrared measurements of SST are not possible in the presence of cloud and hence cloudy data must be identified and removed. A series of tests based on the work of Saunders and Kriebel [1988] are used at RAL to identify cloud contaminated data. Jones et al. [1996] identify the presence of residual cloud contamination (caused by fog, low stratus, and stratocumulus cloud types) in the ASST data and describe a filtering algorithm to reduce this contamination. We use their filtering algorithm to reduce this error source. In brief, the algorithm involves fitting an annual and semi-annual model to the daytime ASST data at each location, and rejecting data that differs from the model by more than three times the standard deviation of the daytime residuals. The ATSR instrument covers the majority of the globe in a 3-day period, however since infrared measurements are not possible in the presence of cloud, it is necessary to average data over a much longer period in order to achieve gap-free SST coverage. As this study focuses on long period (several hundred days) Rossby waves we use monthly averages to reduce the need for interpolation (although during the time of the ERS-1 3- day repeat orbit phase some locations are never sampled due to the track spacing being larger than the 512 km swath width of ATSR). To reduce the effect of residual data spikes we use the median SST within each month. Typically, 3-4 SST values contribute to each monthly average within the North Atlantic region. Remaining gaps are handled by the use of a Gaussian interpolator with Full Width Half Maximum (FWHM) of 100 km and 1 month, and search radii of 300 km and 3 months

We examined SST data for the period January 1992 to December 1995, and calculated anomalies relative to the mean. These are spatially averaged into 1° bins to give monthly 1° SST anomaly maps. As the principal signal in the SST fields is the large scale annual cycle of heating and cooling, a zonal gradient was then taken to emphasise longitudinally propagating signals. These data are depicted in the left hand panel of figure 1.

2.2 ERS-1 altimetry

In this provisional study, we have extracted and processed the altimeter data from phase C (the multi- disciplinary 35-day repeat spanning April 1993 - December 1994). State of the art atmospheric and geophysical corrections are applied, including the most recent Delft orbits whose global rms accuracy is ~5 cm, approaching the high precision of T/P orbits (Scharroo et al., 1997). The CSR3.0 tidal model [Eanes and Bettadpur, 1995] is used to remove the effects of tides. After correction, the SSH data are collocated onto a set of reference latitudes and longitudes. Collocation is by a perpendicular bisector approach [Cheney et al., 1983], and the effects of across-track mean sea surface gradients are removed by using the Basic and Rapp [1992] mean sea surface model. The time-mean SSH is calculated for each point on the reference cycle using the collocated SSH data. This time-mean is then subtracted from individual SSH cycles to obtain the SSH anomaly for each cycle. Finally, the SSH anomalies are gridded onto a 1° by 1° grid by means of Gaussian interpolation using a full- width half-maximum (FWHM) of 150 km and a search radius of 200 km. These parameters were selected empirically. Propagating signals are evident in the longitude-time plots of SSH anomalies at different latitudes [Cipollini et al., 1996a, 1996b]. However, in this study we use the zonal gradient of SSH [Hughes 1995, 1996], which relates directly to the geostrophic currents. This then highlights the presence of Rossby waves and filters out any unwanted large scale signals (including the large scale seasonal steric effect). The use of the zonal gradient is also consistent with the SST data processing (see above) and allows a straightforward comparison of the results. These data are depicted in the central panel of figure 1.

2.3 TOPEX/POSEIDON altimetry

The T/P data used in this study were extracted from the geophysical data records (GDRs) provided on CD-ROMs by Aviso Altimetrie. We extracted the one-second average SSH values in the North Atlantic, covering the period September 1992 to April 1996 (cycles 1 to 132), and applied the standard geophysical corrections [Fu et al., 1994]. Consistent with the ERS-1 data processing, the CSR3.0 tidal model [Eanes and Bettadpur, 1995] is used to remove the effects of tides. The TOPEX dual- frequency ionospheric correction is smoothed with a 21- second moving average before applying it. After correction, the SSH data are collocated onto a set of reference latitudes and longitudes corresponding to cycle 18 (this being a cycle close to the nominal ground track position). SSH anomalies along track and then at the chosen grid points are calculated in an identical manner to that used for ERS-1; the resultant gradients in SSH are depicted in the right hand panel of figure 1.

3. Analysis and discussion

Since Rossby waves propagate mainly zonally it is useful to present SSH gradients in the form of longitude-time plots (detrended in time and space). Propagating waves appear as diagonal features in the plots. Figure 1 reveals a consistent pattern of westward propagating features, some of which can be seen in all three datasets during the time period common to them all. The wavelength, period and propagation speed of the waves can be directly estimated from the plots by visual means. A more objective estimate can be made by evaluating the energy spectrum of the plots using the two-dimensional Fast Fourier Transform (not shown here), which enables various different wavelength and period components to be discerned.

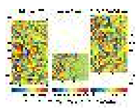

Figure 1 (99 Kbytes)

There is a common 3-year period for which we have processed SSH and SST data from T/P and ATSR respectively. The dominant Fourier peaks in both these fields over the common period are given in Table 1. Each spectrum showed 3 peaks, with other signals not distinguishable from the noise. These are given in order of amplitude, with the corresponding estimates of wavelength l, period T and propagation speed c . A clear agreement is seen in the properties of these 3 peaks, although they are ordered differently in terms of energy. For example, the strongest peak (ssh1) in the SSH dataset has a propagation speed of ~2.6 km/day and appears to correspond with the third strongest peak in SST (sst3). The Radon transform has also been applied to these datasets (Cipollini et al., 1997), yielding similar results, indicating that the results are robust to the type of methodology used.

An analysis of the co-spectra of SSH and SST signals was carried out to determine the coherency and phase lag as a function of frequency. The values of coherency for the corresponding pairs of peaks (see Table 1) were as follows: (ssh1, sst3): 0.52; (ssh2, sst2): 0.60; (ssh3, sst1): 0.57. Coherency estimates at other frequencies - not corresponding to Rossby wave propagation - were all markedly lower than these values. In all three cases, there was no appreciable phase lag, i.e. SSH and SST signals for each propagating wave were found to be in phase.

SSH zonal gradient properties from T/P

peak	l (km)	T (days)	c (km/day)
ssh1	520 (470-570)	200 (180-220)	2.6 (2.1-3.2)
ssh2	380 (360-410)	240 (220-290)	1.6 (1.2-1.9)
ssh3	390 (360-410)	490 (400-670)	0.8 (0.5-1.0)

SST zonal gradient properties from ATSR

peak	l (km)	T (days)	c (km/day)

sst1	390 (360-420)	480 (390-630)	0.8 (0.6-1.1)
sst2	380 (350-400)	240 (210-270)	1.6 (1.3-1.9)
sst3	510 (470-560)	190 (175-210)	2.7 (2.2-3.2)

Table 1. Signal properties of the strongest signals in the T/P SSH and ATSR SST datasets. The values of wavelength l are estimated by weighted linear interpolation in the wavenumber domain. The values of period T correspond to the frequency of the spectral bin in the FFT. All quantities are given together with the range of possible values (based on spectral resolution) in brackets.

In the whole analysis, which will be the subject of a future paper, we have considered longitude-time plots and their spectra in the North Atlantic between 20°N and 46°N. We observe that Rossby wave characteristics tend to change when the waves cross the Mid-Atlantic Ridge into the western sub-basin [Tokmakian and Challenor, 1993; Cipollini et al., 1996b]. For each value of the latitude, two spans of 31 degrees in longitude (east and west of the ridge) were chosen as a good compromise between wavenumber resolution and homogeneity of the wave propagation characteristics. Here, we focus only on some results obtained east of the ridge at 34°N, where the propagating signals present some peculiarities that would suggest an active role by the Azores Current which flows at that latitude. Since we have not yet investigated the spectral properties of the ERS-1 altimeter data, the analysis presented here concentrates just on the T/P SSH and ATSR SST datasets, as reported by Cipollini et al., 1997. However, it is worth noting that the potential for detection of long- wavelength baroclinic Rossby waves in ERS-1 altimetry is very clear. We intend to include the second 35-day repeat phase as well as ERS-2 altimetry in future work.

Le Traon and De Mey [1994] have already observed in Geosat data some well defined wave-like structures propagating westward at the latitude of the Azores Current, and suggest that such features could be "waves generated in the east which interact with the Azores front in winter and trigger its meandering". Indeed, the same authors assume a Rossby wave structure for the waves. Cipollini et al. [1996b, 1997] have observed from T/P data that the most energetic wave signals, having characteristics which match those of Rossby waves, are found at 33°N and 34°N. Figure 1 (right hand panel) shows the longitude-time plot of the T/P SSH zonal gradients at 34°N. The diagonal signals in this plot indicate that Rossby waves are generated close to the eastern boundary and propagate to the west. In a separate study, we have examined the spectrum of these data (Cipollini et al., 1997). The properties of the periodic signals corresponding to the strongest peaks are given in descending order of energy in Table 1.

In summary, we appear to observe three distinct propagation speeds: ~2.7, ~1.6 and 0.8 km/day. We suggest that the fastest speed corresponds to the first- mode baroclinic Rossby wave and, more tentatively, the slower two speeds to the second and third baroclinic modes. In altimetry, the fastest observed baroclinic mode is the most energetic, and the slowest is the least energetic. In temperature, the order is reversed.

The observed SST/SSH ratios are: $\rho'/p' \approx$ 3.7, 5.4, 6.6 for the 3 modes. Why should this be so? Theory (P. Killworth, personal communication, 1996) suggests that the near-surface density balance is time change vs. northwards advection against a mean density gradient:

$$(\overline{u}-c)\rho' + v'\rho_y \approx 0$$

Thus $T'/h' \propto \overline{u}_Z/\alpha(\overline{u}-c)$. Using observed $\overline{u}$ and c for modes, and using "effective expansion coefficient of heat" gives very similar ratios for the observed and predicted ratios of SST/SSH.

Outside the preferred zonal band of propagation at 33°-34°N, the agreement between SSH and SST gradients is weaker. One reason for this, at least for some regions of the North Atlantic, could be the strong signature of mesoscale activity in the SST field which tends to mask Rossby wave propagation. On the other hand, the large amplitude of the signals at the latitude of the present study, and the fact that they are so clearly observable in both fields, suggests that the interaction between the Azores Current and the waves could be such as to amplify the waves. This "waveguide effect" has been observed in the Antarctic Circumpolar Current [Hughes, 1996].

4. Summary and conclusions

This paper exploits the synergism of satellite remote sensing of more than one geophysical variable to present evidence for propagating Rossby waves from SSH and SST datasets collected in the same ocean region over an overlapping time period. We have focussed on combined observations of long-wavelength baroclinic Rossby waves in the Northeast Atlantic (east of the Mid-Atlantic Ridge) in both SSH and SST using TOPEX/POSEIDON altimetry and the ERS-1 ATSR. Consistent features are also observed in the first ERS-1 35-day repeat phase altimeter dataset. Examination of the longitude-time plots and of their energy spectra reveals a remarkable correspondence in propagating features, at least in a zonal band near 34°N. In both T/P SSH and ATSR SST zonal gradient datasets, we appear to observe three distinct speeds: ~2.7, ~1.6 and ~0.8 km/day, which may correspond to the first three baroclinic modes of Rossby wave propagation. The values of speed we observe at this and other latitudes for the first-mode baroclinic Rossby wave are consistent with a revised theory of Rossby wave propagation [Killworth et al., 1997] which has recently been introduced to explain the observed discrepancy [Chelton and Schlax, 1996] between altimeter-derived wave speeds and those computed from the standard linear theory. It is worth pointing out that examination of latitude-time plots re- veals little evidence of a north-south component to Rossby wave propagation in our area of interest. Therefore, the assumption of zonal wave propagation is reasonable.

Although data smoothing and interpolation can sometimes lead to misinterpretation of mapped features, it should be borne in mind that we have presented data from three different sensors on two different platforms with different spatial and temporal sampling characteristics which have yielded results remarkably consistent with Rossby wave propagation. Nonetheless, we intend to employ additional approaches in a future paper including the use of 3D spatial-temporal autocorrelation functions as presented by Glazman et al. [1996], thus circumventing the need to grid data. This will have the added benefit of yielding both the zonal and meridional wavenumbers of Rossby wave propagation.

This paper shows that it is possible, at least in some energetic regions, to observe Rossby waves both with altimetry and infrared measurements. Further studies are now needed to explain more fully the Rossby wave characteristics inferred from both SSH and SST datasets, as well as to explain the interaction effect observed between the waves and the Azores Current.

5. Acknowledgements

We are grateful to the T/P team and Aviso Altimetrie for provision of the T/P altimeter data, ESA for the provision of the ERS-1 data, and Chris Mutlow, Albin Závody, and the ATSR Science team at RAL for the ASST data. We thank Helen Snaith for her contributions to the altimeter data processing software, Peter Killworth for encouragement and discussion, and Giovanni Corsini for advice on spectral analysis. Paolo Cipollini is supported by the Commission of European Communities through a Research Training Fellowship (HCM contract no. ERBCHBGCT930440); Matthew Jones is funded by Natural Environment Research Council grant GR3/10796.

6. References

Andersen O.B., P.L. Woodworth and R.A. Flather, 1995:
Intercomparison of recent ocean tide models, *J. Geophys. Res.*, **100**, 25261-25282.
ATSR home page:
http://www.atsr.rl.ac.uk/
Basic, T. and R.H. Rapp, 1992:
Oceanwide prediction of gravity anomalies and sea surface heights using Geos-3, Seasat and Geosat altimeter data and ETOPO5U bathymetric data, Rep.416, Dept. Geod. Sci. Surv., The Ohio State University, Columbus.
Cheney, R.E., J.G. Marsh and B.D. Beckley, 1983:
Global mesoscale variability from collinear tracks of SEASAT altimeter data, *J. Geophys. Res.*, **88**, 4343- 4354.
Chelton, D.B. and M.G. Schlax, 1996:
Global observation of oceanic Rossby waves, *Science*, **272**, 234-238.
Cipollini, P., D. Cromwell and G.D. Quartly, 1996a:
Observations of Rossby Wave Propagation in the Northeast Atlantic with Topex/Poseidon Altimetry, submitted to *Adv. Space Res.* - PDF version (122 Kbytes)
Cipollini, P., D. Cromwell and G.D. Quartly, 1996b:
Variability of Rossby wave propagation in the North Atlantic from TOPEX/POSEIDON altimetry, *Proc. IGARSS '96*, Lincoln, Nebraska, vol. I, 91-93.
Cipollini, P., D. Cromwell, M.S. Jones, G.D. Quartly and P. G. Challenor, 1997:
Concurrent TOPEX/POSEIDON altimeter and Along-Track Scanning Radiometer observations of Rossby wave propagation near 34°N in the Northeast Atlantic, *Geophys. Res. Letters*, **24**, 889-892.
Delft precise orbits - web page:
http://dutlru8.lr.tudelft.nl/ers/precorbs/
Eanes, R.J. and S.V. Bettadpur, 1995:
The CSR 3.0 global ocean tide model: diurnal and semi-diurnal ocean tides from TOPEX/POSEIDON altimetry, CSR Tech. Memo. 95-06, Center for Space Research, The University of Texas at Austin, Texas.
Forrester, T.N. and P.G. Challenor, 1995:
Validation of ATSR sea surface temperatures in the Færoes region, *Int. J. Rem. Sens.*, **16**, 2741-2753.
Fu, L.-L., E.J. Christensen, C.A. Yamarone, M. Lefebvre, Y. Menard, M. Dorrer and P. Escudier, 1994:
TOPEX/POSEIDON mission overview, *J. Geophys. Res.*, **99**, 24,369-24,381.
Gill, A.E., 1982:
Atmosphere-Ocean Dynamics, 662pp., Academic Press, San Diego.
Glazman, R.E., A. Fabrikant and A. Greysukh, 1996:
Statistics of spatial-temporal variations of sea surface height based on TOPEX altimeter measurements, *Int. J. Remote Sensing*, **17**, 2647-2666.
Halliwell, G.R. Jr., Y.J. Ro and P. Cornillon, 1991:
Westward-propagating SST anomalies and baroclinic eddies in the Sargasso sea, *J. Phys. Oceanogr.*, **21**, 1664-1679.
Hughes, C.W., 1995:
Rossby Waves in the Southern Ocean: A comparison of TOPEX/POSEIDON altimetry with model predictions. *J. Geophys. Res*, **100**, 15,933-15,950.
Hughes, C.W., 1996:
The Antarctic Circumpolar Current as a waveguide for Rossby waves, *J. Phys. Oceanogr.*, **26**, 1375-1387.
Jacobs, G.A., H.E. Hurlburt, J.C. Kindle, E.J. Metzger, J.L. Mitchell, W.J. Teague and A.J. Wallcraft, 1994:
Decade-scale trans-Pacific propagation and warming effects of an El Nio anomaly, *Nature*, **370**, 360-363.
Jones, M.S., M.A. Saunders and T.H. Guymer, 1996:
Global remnant cloud contamination in the Along-Track Scanning Radiometer data: Source and removal, *J. Geophys. Res.*, **101**, 12141-12147.
Killworth, P., D.B. Chelton and R. deSzoeke, 1997:
The speed of observed and theoretical long extra- tropical planetary waves, *J. Phys. Ocean.*, in press.
Le Traon, P.-Y. and P. De Mey, 1994:
The eddy field associated with the Azores Front east of the Mid- Atlantic Ridge as observed by the Geosat altimeter, *J. Geophys. Res.*, **99**, 9907-9923.
McClain, E.P., W.G. Pichel and C.C. Walton, 1985:
Comparative performance of AVHRR-based multichannel sea surface temperatures, *J. Geophys. Res.*, **90**, 11587-11601.
Mutlow, C.T., A.M. Závody, I.J. Barton and D.T. Llewellyn-Jones, 1994:
Sea surface temperature measurements by the Along-Track Scanning Radiometer on the ERS-1 satellite: Early results., *J. Geophys. Res.*, **99**, 22,575-22,588.
Saunders, R.W. and K.T. Kriebel, 1988:
An improved method for detecting clear sky and cloudy radiances from AVHRR data. *Int. J. Remote Sensing*, **9**, 123-150 & 1393-1394.
Schlax, M.G. and D.B. Chelton, 1994:
Aliased tidal errors in TOPEX/POSEIDON sea surface height data, *J. Geophys. Res.*, **99**, 24761-24775.
Scharroo R., P. Visser and G. Mets, 1997:
TOPEX-class Orbits for the ERS Satellites, submitted to *J. Geophys. Res.* - Postscript version of the preprint (2.7 Mbytes)
Tokmakian, R.T. and P.G. Challenor, 1993:
Observations in the Canary Basin and the Azores Frontal Region using Geosat data, *J. Geophys. Res.*, **98**, 4761-4773.
Van Woert, M.L. and J.M. Price, 1993:
Geosat and Advanced Very High Resolution Radiometer observations of oceanic planetary waves adjacent to the Hawaiian Islands, *J. Geophys. Res.*, **98**, 14,619-14,631.
Závody, A.M., C.T. Mutlow and D.T. Llewellyn-Jones, 1995:
A radiative transfer model for sea surface temperature retrieval for the Along-Track Scanning Radiometer, *J. Geophys. Res.*, **100**, 937-952.

Keywords: ESA European Space Agency - Agence spatiale europeenne, observation de la terre, earth observation, satellite remote sensing, teledetection, geophysique, altimetrie, radar, chimique atmospherique, geophysics, altimetry, radar, atmospheric chemistry